

On electromagnetic surface waves supported by an isotropic chiral material

James Noonan¹ and Tom G. Mackay^{1,2,*}

¹*School of Mathematics and Maxwell Institute for Mathematical Sciences,
University of Edinburgh, Edinburgh EH9 3JZ, United Kingdom*

²*NanoMM—Nanoengineered Metamaterials Group, Department of Engineering Science and
Mechanics, Pennsylvania State University, University Park, PA 16802–6812, USA*

Abstract

Electromagnetic surface waves supported by an isotropic chiral material were investigated via the associated canonical boundary-value problem. Specifically, two scenarios were considered: surface waves guided by the planar interface of an isotropic chiral material and (a) an isotropic dielectric material and (b) a uniaxial dielectric (or plasmonic) material. Both plasmonic and non-plasmonic achiral partnering materials were investigated. In scenario (a) surface waves akin to surface-plasmon-polariton (SPP) waves were excited, while in scenario (b) surface waves akin to Dyakonov waves and akin to SPP waves were excited. For numerical studies, an isotropic chiral material capable of simultaneously supporting attenuation and amplification of plane waves, depending upon circular polarization state, was used. The amplitude of the SPP-like waves could be either amplified or attenuated, depending upon the relative permittivity of the isotropic dielectric partnering material for scenario (a), or depending upon the direction of propagation relative to the optic axis of the uniaxial dielectric partnering material for scenario (b).

Keywords: isotropic chiral material, surface plasmon polariton wave, Dyakonov wave

1 Introduction

The planar interface of two dissimilar materials can guide the propagation of electromagnetic surface waves. A variety of different types of electromagnetic surface wave have been identified, with the type depending upon whether the partnering materials are isotropic or anisotropic, dissipative or nondissipative, homogeneous or nonhomogeneous, and so forth [1]. The surface-plasmon-polariton (SPP) wave [2, 3] — which is guided by the planar interface of a metal and a dielectric material — is the most familiar type of electromagnetic surface wave, being widely exploited in optical sensing applications [4, 5]. The Dyakonov surface wave [6] — which is guided by the planar interface of an isotropic dielectric material and an anisotropic dielectric material — has also been widely reported upon [7, 8]. Dyakonov waves are promising for applications in optical communications [9].

As compared to achiral materials, chiral materials [10] — with their inherent magnetoelectric coupling — offer wider opportunities for surface-wave propagation. However, whereas surface waves guided by planar interfaces involving achiral partnering materials have been comprehensively studied, there have been only a

*Corresponding author. E-mail: T.Mackay@ed.ac.uk

few studies of the surface waves supported by chiral materials [11–14]. And these few studies have largely focussed on isotropic partnering materials and nondissipative chiral materials. In the present paper we address this issue by investigating surface waves supported by a chiral material with the effects of dissipation and anisotropy of the partnering materials being taken into account. In particular, a novel type of chiral material that can simultaneously support attenuation and amplification of plane waves [15], depending upon circular polarization state, is considered. Our theoretical and numerical studies are based on the canonical boundary-value problem for surface-wave propagation [1].

In the following, the permittivity and permeability of free space are written as ε_0 and μ_0 , respectively. The free-space wavenumber is $k_0 = \omega\sqrt{\varepsilon_0\mu_0}$, where ω is the angular frequency. The operators $\text{Re}\{\cdot\}$ and $\text{Im}\{\cdot\}$ deliver the real and imaginary parts of complex-valued quantities, and $i = \sqrt{-1}$. Single underlining signifies a 3 vector while double underlining signifies a 3×3 dyadic. The triad of unit vectors aligned with the Cartesian axes are denoted as $\{\underline{\hat{u}}_x, \underline{\hat{u}}_y, \underline{\hat{u}}_z\}$.

2 Isotropic chiral material/isotropic dielectric material interface

Let us consider the canonical boundary-value problem for surface waves guided by the planar interface of an isotropic chiral material and an isotropic dielectric material. Both partnering materials are homogeneous. The isotropic chiral material, labeled \mathcal{A} , fills the half-space $z > 0$ and is characterized by the frequency-domain Tellegen constitutive relations [10]

$$\left. \begin{aligned} \underline{D}(\underline{r}) &= \varepsilon_0\varepsilon_{\mathcal{A}}\underline{E}(\underline{r}) + i\sqrt{\varepsilon_0\mu_0}\xi_{\mathcal{A}}\underline{H}(\underline{r}) \\ \underline{B}(\underline{r}) &= -i\sqrt{\varepsilon_0\mu_0}\xi_{\mathcal{A}}\underline{E}(\underline{r}) + \mu_0\mu_{\mathcal{A}}\underline{H}(\underline{r}) \end{aligned} \right\} \quad z > 0. \quad (1)$$

The relative permittivity scalar $\varepsilon_{\mathcal{A}}$, the relative permeability scalar $\mu_{\mathcal{A}}$, and the relative chirality pseudoscalar $\xi_{\mathcal{A}}$ are frequency dependent and complex valued, per the principle of causality embodied by the Kramers–Kronig relations [16]. The isotropic dielectric material, labeled \mathcal{B} , fills the half-space $z < 0$ and is characterized by the relative permittivity $\varepsilon_{\mathcal{B}}$.

2.1 Theory

The electromagnetic field phasors in the partnering materials \mathcal{A} and \mathcal{B} are represented by

$$\left. \begin{aligned} \underline{E}_{\ell}(\underline{r}) &= \underline{\mathcal{E}}_{\ell} \exp(i\underline{k}_{\ell} \cdot \underline{r}) \\ \underline{H}_{\ell}(\underline{r}) &= \underline{\mathcal{H}}_{\ell} \exp(i\underline{k}_{\ell} \cdot \underline{r}) \end{aligned} \right\}, \quad \ell \in \{\mathcal{A}, \mathcal{B}\}. \quad (2)$$

The amplitude vectors $\underline{\mathcal{E}}_{\ell}$ and $\underline{\mathcal{H}}_{\ell}$ have complex-valued components, and so does the wave vector \underline{k}_{ℓ} . The field phasors (and the wave vector) can vary with angular frequency ω . Without loss of generality, we consider the surface-wave propagation parallel to $\underline{\hat{u}}_x$ in the xy plane; i.e., $\underline{\hat{u}}_y \cdot \underline{k}_{\ell} \equiv 0$.

In the half-space $z > 0$, the Maxwell curl postulates yield

$$\left. \begin{aligned} \underline{k}_{\mathcal{A}} \times \underline{\mathcal{E}}_{\mathcal{A}} - \omega(-i\sqrt{\varepsilon_0\mu_0}\xi_{\mathcal{A}}\underline{\mathcal{E}}_{\mathcal{A}} + \mu_0\mu_{\mathcal{A}}\underline{\mathcal{H}}_{\mathcal{A}}) &= \underline{0} \\ \underline{k}_{\mathcal{A}} \times \underline{\mathcal{H}}_{\mathcal{A}} + \omega(\varepsilon_0\varepsilon_{\mathcal{A}}\underline{\mathcal{E}}_{\mathcal{A}} + i\sqrt{\varepsilon_0\mu_0}\xi_{\mathcal{A}}\underline{\mathcal{H}}_{\mathcal{A}}) &= \underline{0} \end{aligned} \right\}, \quad (3)$$

where the wave vector

$$\underline{k}_{\mathcal{A}} = k_0(q\underline{\hat{u}}_x + i\alpha_{\mathcal{A}}\underline{\hat{u}}_z) \quad (4)$$

and $\text{Re}\{\alpha_{\mathcal{A}}\} > 0$ for surface-wave propagation. On combining Eqs. (3) and Eq. (4), a biquadratic dispersion relation emerges for $\alpha_{\mathcal{A}}$. The two $\alpha_{\mathcal{A}}$ roots with non-negative real parts are identified as

$$\left. \begin{aligned} \alpha_{\mathcal{A}1} &= \sqrt{q^2 - \kappa_R^2} \\ \alpha_{\mathcal{A}2} &= \sqrt{q^2 - \kappa_L^2} \end{aligned} \right\}, \quad (5)$$

with the complex-valued scalars

$$\left. \begin{aligned} \kappa_R &= \sqrt{\varepsilon_{\mathcal{A}}\mu_{\mathcal{A}}} + \xi_{\mathcal{A}} \\ \kappa_L &= \sqrt{\varepsilon_{\mathcal{A}}\mu_{\mathcal{A}}} - \xi_{\mathcal{A}} \end{aligned} \right\} \quad (6)$$

being associated with the relative wave numbers for right and left circularly-polarized light in an unbounded chiral medium [10]. Accordingly the field-phasor amplitudes are given as

$$\left. \begin{aligned} \underline{\mathcal{E}}_{\mathcal{A}} &= A_{\mathcal{A}1} \underline{\mathcal{E}}_{\mathcal{A}1} + A_{\mathcal{A}2} \underline{\mathcal{E}}_{\mathcal{A}2} \\ \underline{\mathcal{H}}_{\mathcal{A}} &= \sqrt{\frac{\varepsilon_0}{\mu_0}} \sqrt{\frac{\varepsilon_{\mathcal{A}}}{\mu_{\mathcal{A}}}} (A_{\mathcal{A}1} \underline{\mathcal{H}}_{\mathcal{A}1} + A_{\mathcal{A}2} \underline{\mathcal{H}}_{\mathcal{A}2}) \end{aligned} \right\}, \quad (7)$$

where the vectors

$$\left. \begin{aligned} \underline{\mathcal{E}}_{\mathcal{A}1} &= \alpha_{\mathcal{A}1} \hat{u}_x + \kappa_R \hat{u}_y + iq \hat{u}_z \\ \underline{\mathcal{E}}_{\mathcal{A}2} &= -\alpha_{\mathcal{A}2} \hat{u}_x + \kappa_L \hat{u}_y - iq \hat{u}_z \\ \underline{\mathcal{H}}_{\mathcal{A}1} &= -i\alpha_{\mathcal{A}1} \hat{u}_x - i\kappa_R \hat{u}_y + q \hat{u}_z \\ \underline{\mathcal{H}}_{\mathcal{A}2} &= -i\alpha_{\mathcal{A}2} \hat{u}_x + i\kappa_L \hat{u}_y + q \hat{u}_z \end{aligned} \right\}. \quad (8)$$

In the half-space $z < 0$, the Maxwell curl postulates yield

$$\left. \begin{aligned} \underline{k}_{\mathcal{B}} \times \underline{\mathcal{E}}_{\mathcal{B}} - \omega\mu_0 \underline{\mathcal{H}}_{\mathcal{B}} &= \underline{0} \\ \underline{k}_{\mathcal{B}} \times \underline{\mathcal{H}}_{\mathcal{B}} + \omega\varepsilon_0 \varepsilon_{\mathcal{B}} \underline{\mathcal{E}}_{\mathcal{B}} &= \underline{0} \end{aligned} \right\}, \quad (9)$$

where the wave vector

$$\underline{k}_{\mathcal{B}} = k_0 (q \hat{u}_x - i\alpha_{\mathcal{B}} \hat{u}_z), \quad (10)$$

and the scalar

$$\alpha_{\mathcal{B}} = \sqrt{q^2 - \varepsilon_{\mathcal{B}}} \quad (11)$$

satisfies the inequality $\text{Re}\{\alpha_{\mathcal{B}}\} > 0$ for surface-wave propagation. Hence the field-phasor amplitudes are given as

$$\left. \begin{aligned} \underline{\mathcal{E}}_{\mathcal{B}} &= A_{\mathcal{B}1} \hat{u}_y + A_{\mathcal{B}2} (i\alpha_{\mathcal{B}} \hat{u}_x + q \hat{u}_z) \\ \underline{\mathcal{H}}_{\mathcal{B}} &= \sqrt{\frac{\varepsilon_0}{\mu_0}} [A_{\mathcal{B}1} (i\alpha_{\mathcal{B}} \hat{u}_x + q \hat{u}_z) - A_{\mathcal{B}2} \varepsilon_{\mathcal{B}} \hat{u}_y] \end{aligned} \right\}. \quad (12)$$

The scalars $A_{\mathcal{A}1}$ and $A_{\mathcal{A}2}$ in Eqs. (7), and $A_{\mathcal{B}1}$ and $A_{\mathcal{B}2}$ in Eqs. (12), as well as the relative wave number q , are determined by enforcing boundary conditions across the planar interface $z = 0$, as follows. The continuity of tangential components of the electric and magnetic field phasors across the planar interface $z = 0$ imposes the four conditions [17]

$$\left. \begin{aligned} \alpha_{\mathcal{A}1} A_{\mathcal{A}1} - \alpha_{\mathcal{A}2} A_{\mathcal{A}2} &= i\alpha_{\mathcal{B}} A_{\mathcal{B}2} \\ \kappa_R A_{\mathcal{A}1} + \kappa_L A_{\mathcal{A}2} &= A_{\mathcal{B}1} \\ -\sqrt{\varepsilon_{\mathcal{A}}} (\alpha_{\mathcal{A}1} A_{\mathcal{A}1} + \alpha_{\mathcal{A}2} A_{\mathcal{A}2}) &= \alpha_{\mathcal{B}} \sqrt{\mu_{\mathcal{A}}} A_{\mathcal{B}1} \\ \sqrt{\varepsilon_{\mathcal{A}}} (\kappa_R A_{\mathcal{A}1} - \kappa_L A_{\mathcal{A}2}) &= -i\varepsilon_{\mathcal{B}} \sqrt{\mu_{\mathcal{A}}} A_{\mathcal{B}2} \end{aligned} \right\}. \quad (13)$$

The four conditions (13) may be represented compactly as

$$[M] \cdot \begin{bmatrix} A_{\mathcal{A}1} \\ A_{\mathcal{A}2} \\ A_{\mathcal{B}1} \\ A_{\mathcal{B}2} \end{bmatrix} = \begin{bmatrix} 0 \\ 0 \\ 0 \\ 0 \end{bmatrix}, \quad (14)$$

wherein the 4×4 matrix $[M]$ must be singular for surface-wave propagation. The dispersion equation $\det [M] = 0$ reduces to the equation

$$2\sqrt{\varepsilon_{\mathcal{A}}\mu_{\mathcal{A}}}\left(\alpha_{\mathcal{A}1}\alpha_{\mathcal{A}2}\varepsilon_{\mathcal{B}} + \kappa_L\kappa_R\alpha_{\mathcal{B}}^2\right) + \alpha_{\mathcal{B}}\left(\kappa_L\alpha_{\mathcal{A}1} + \kappa_R\alpha_{\mathcal{A}2}\right)\left(\varepsilon_{\mathcal{A}} + \varepsilon_{\mathcal{B}}\mu_{\mathcal{A}}\right) = 0, \quad (15)$$

from which q may be extracted, generally by numerical means. Once q is known, relative values of the four scalars $A_{\mathcal{A}1,2}$ and $A_{\mathcal{B}1,2}$ can be determined from Eq. (14) by straightforward algebraic manipulations.

2.2 Numerical studies

For our numerical studies we fix partnering material \mathcal{A} by selecting the relative constitutive parameters $\varepsilon_{\mathcal{A}} = 2.6724 - 0.0007i$, $\xi_{\mathcal{A}} = 0.0652 + 0.0005i$ and $\mu_{\mathcal{A}} = 0.9642 + 0.0001i$. These parameters prescribe a homogenized composite material that arises from blending together a realistic isotropic chiral material with an active dielectric material, namely a rhodamine mixture [15]. The constitutive parameters of the homogenized composite material were estimated using the Bruggeman formalism [18]. For material \mathcal{A} , the relative wave numbers are $\kappa_L = 1.5401 - 0.0006i$ and $\kappa_R = 1.6705 + 0.0004i$. Therefore, if material \mathcal{A} were unbounded it would simultaneously support the amplification of left circularly-polarized plane waves and the attenuation of right circularly-polarized plane waves [15]. Parenthetically, in a similar vein, anisotropic dielectric materials can be engineered that amplify plane waves of one linearly-polarized state but attenuate plane waves of the other linearly-polarized state [19].

Let us begin by considering the case wherein partnering material \mathcal{B} is characterized by a real-valued relative permittivity with $\varepsilon_{\mathcal{B}} < 0$. That is, material \mathcal{B} behaves like an idealized plasmonic material and the corresponding surface waves are akin to Fano waves [1, 20]. The dispersion equation (15) then yields one (complex-valued) q solution. The real and imaginary parts of the relative wave number q are plotted against relative permittivity $\varepsilon_{\mathcal{B}}$ in Fig. 1. While the real part of q remains almost constant as $\varepsilon_{\mathcal{B}}$ is increased, the imaginary part of q undergoes a much more dramatic change. In particular, $\text{Im}\{q\}$ is positive valued for $\varepsilon_{\mathcal{B}} < -21$ but is negative valued for $\varepsilon_{\mathcal{B}} > -21$. Therefore, for sufficiently small values of $\varepsilon_{\mathcal{B}}$ the surface wave is attenuated as it propagates whereas for larger values of $\varepsilon_{\mathcal{B}}$ the surface wave is amplified as it propagates.

We explore this behaviour further, in a more realistic setting, by supposing that partnering material \mathcal{B} exhibits a small degree of dissipation. That is, we fix $\text{Re}\{\varepsilon_{\mathcal{B}}\} = -10$ and consider $\text{Im}\{\varepsilon_{\mathcal{B}}\} > 0$. Accordingly, material \mathcal{B} behaves like a realistic plasmonic material and the corresponding surface waves are akin to SPP waves [21, 22]. As for the case represented in Fig. 1, the dispersion equation (15) delivers a single (complex-valued) q solution. The real and imaginary parts of the relative wave number q are plotted against the imaginary part of the relative permittivity $\varepsilon_{\mathcal{B}}$ in Fig. 2. The real part of q is almost independent of $\text{Im}\{\varepsilon_{\mathcal{B}}\}$ over the range considered in Fig. 2. In contrast, for $\text{Im}\{\varepsilon_{\mathcal{B}}\} < 0.005$ we have $\text{Im}\{q\} < 0$ whereas for $\text{Im}\{\varepsilon_{\mathcal{B}}\} > 0.005$ we have $\text{Im}\{q\} > 0$. Therefore, when the degree of dissipation exhibited by material \mathcal{B} is sufficiently small the surface wave is amplified, but when the degree of dissipation exhibited by material \mathcal{B} is larger the surface wave is attenuated.

Next we turn to the case where $\text{Re}\{\varepsilon_{\mathcal{B}}\} > 0$. Specifically, let $\text{Re}\{\varepsilon_{\mathcal{B}}\} = 10$. Notice that in this case partnering material \mathcal{B} does not behave like a plasmonic material and the corresponding surface waves are not at all akin to SPP waves. In Fig. 3, the real and imaginary parts of q are plotted against $\text{Im}\{\varepsilon_{\mathcal{B}}\}$, for the single (complex-valued) solution emerging from the dispersion equation (15) for $\text{Im}\{\varepsilon_{\mathcal{B}}\} > 0.05$. The real part of q is almost independent of $\text{Im}\{\varepsilon_{\mathcal{B}}\}$ whereas the imaginary part of q increases approximately linearly as $\text{Im}\{\varepsilon_{\mathcal{B}}\}$ increases. Since $\text{Im}\{q\} > 0$, the corresponding surface wave is attenuated over the range of values of $\text{Im}\{\varepsilon_{\mathcal{B}}\}$ considered. If $0 \leq \text{Im}\{\varepsilon_{\mathcal{B}}\} < 0.05$ then no solutions emerge from the dispersion equation (15). In particular, no solutions are found when material \mathcal{B} is nondissipative and $\varepsilon_{\mathcal{B}} > 0$, a result that is consistent with an earlier study [13].

3 Isotropic chiral material/anisotropic dielectric material interface

Now we extend the canonical boundary-value problem presented in Sec. 2 by replacing the isotropic dielectric material, i.e., partnering material \mathcal{B} , with an anisotropic dielectric material. Partnering material \mathcal{A} is still taken to be an isotropic chiral material, per the Tellegen constitutive relations (1). To be specific, partnering material \mathcal{B} is taken to be a uniaxial dielectric material characterized by the relative permittivity dyadic [17]

$$\underline{\underline{\varepsilon}}_{\mathcal{B}} = \varepsilon_{\mathcal{B}}^s \underline{\underline{I}} + (\varepsilon_{\mathcal{B}}^t - \varepsilon_{\mathcal{B}}^s) \hat{\underline{u}} \hat{\underline{u}}, \quad (16)$$

where $\underline{\underline{I}} = \hat{\underline{u}}_x \hat{\underline{u}}_x + \hat{\underline{u}}_y \hat{\underline{u}}_y + \hat{\underline{u}}_z \hat{\underline{u}}_z$ is the identity dyadic. The optic axis of material \mathcal{B} lies in the xy plane, oriented at angle ψ with respect to the direction of surface-wave propagation; i.e.,

$$\hat{\underline{u}} = \cos \psi \hat{\underline{u}}_x + \sin \psi \hat{\underline{u}}_y. \quad (17)$$

The dyadic $\underline{\underline{\varepsilon}}_{\mathcal{B}}$ has two eigenvalues: $\varepsilon_{\mathcal{B}}^s$ which governs the propagation of *ordinary* plane waves and $\varepsilon_{\mathcal{B}}^t$ which, together with $\varepsilon_{\mathcal{B}}^s$, governs the propagation of *extraordinary* plane waves [23].

3.1 Theory

In the half-space $z > 0$, Eqs. (3)–(8) continue to hold. In the half-space $z < 0$, the Maxwell curl postulates yield

$$\left. \begin{aligned} \underline{k}_{\mathcal{B}} \times \underline{\mathcal{E}}_{\mathcal{B}} &= \omega \mu_0 \underline{\mathcal{H}}_{\mathcal{B}} \\ \underline{k}_{\mathcal{B}} \times \underline{\mathcal{H}}_{\mathcal{B}} &= -\omega \varepsilon_0 \underline{\underline{\varepsilon}}_{\mathcal{B}} \cdot \underline{\mathcal{E}}_{\mathcal{B}} \end{aligned} \right\}, \quad (18)$$

where the wave vector $\underline{k}_{\mathcal{B}}$ has the form given in Eq. (10). The combination of Eqs. (18) and Eq. (10) yields a biquadratic dispersion relation for $\alpha_{\mathcal{B}}$. For surface-wave propagation the two $\alpha_{\mathcal{B}}$ roots with non-negative real parts are prescribed; these are

$$\left. \begin{aligned} \alpha_{\mathcal{B}1} &= \sqrt{q^2 - \varepsilon_{\mathcal{B}}^s} \\ \alpha_{\mathcal{B}2} &= \sqrt{\varepsilon_{\mathcal{B}}^t \left[q^2 \left(\frac{\cos^2 \psi}{\varepsilon_{\mathcal{B}}^s} + \frac{\sin^2 \psi}{\varepsilon_{\mathcal{B}}^t} \right) - 1 \right]} \end{aligned} \right\}. \quad (19)$$

Hence the field phasor amplitudes for $z < 0$ are

$$\left. \begin{aligned} \underline{\mathcal{E}}_{\mathcal{B}} &= A_{\mathcal{B}1} \underline{\mathcal{E}}_{\mathcal{B}1} + A_{\mathcal{B}2} \underline{\mathcal{E}}_{\mathcal{B}2} \\ \underline{\mathcal{H}}_{\mathcal{B}} &= \sqrt{\frac{\varepsilon_0}{\mu_0}} (A_{\mathcal{B}1} \underline{\mathcal{H}}_{\mathcal{B}1} + A_{\mathcal{B}2} \underline{\mathcal{H}}_{\mathcal{B}2}) \end{aligned} \right\}, \quad (20)$$

where the vectors

$$\left. \begin{aligned} \underline{\mathcal{E}}_{\mathcal{B}1} &= i\alpha_{\mathcal{B}1} \sin \psi \hat{\underline{u}}_x - i\alpha_{\mathcal{B}1} \cos \psi \hat{\underline{u}}_y + q \sin \psi \hat{\underline{u}}_z \\ \underline{\mathcal{E}}_{\mathcal{B}2} &= \alpha_{\mathcal{B}1}^2 \cos \psi \hat{\underline{u}}_x - \varepsilon_{\mathcal{B}}^s \sin \psi \hat{\underline{u}}_y - iq\alpha_{\mathcal{B}2} \cos \psi \hat{\underline{u}}_z \\ \underline{\mathcal{H}}_{\mathcal{B}1} &= \alpha_{\mathcal{B}1}^2 \cos \psi \hat{\underline{u}}_x - \varepsilon_{\mathcal{B}}^s \sin \psi \hat{\underline{u}}_y - i\alpha_{\mathcal{B}1} q \cos \psi \hat{\underline{u}}_z \\ \underline{\mathcal{H}}_{\mathcal{B}2} &= -i\alpha_{\mathcal{B}2} \varepsilon_{\mathcal{B}}^s \sin \psi \hat{\underline{u}}_x + i\alpha_{\mathcal{B}2} \varepsilon_{\mathcal{B}}^s \cos \psi \hat{\underline{u}}_y - \varepsilon_{\mathcal{B}}^s q \sin \psi \hat{\underline{u}}_z \end{aligned} \right\}. \quad (21)$$

As in Sec. 2, the scalars $A_{\mathcal{A}1}$ and $A_{\mathcal{A}2}$ in Eqs. (7), and $A_{\mathcal{B}1}$ and $A_{\mathcal{B}2}$ in Eqs. (20), as well as the wave number q , are determined by enforcing boundary conditions across the planar interface $z = 0$. To this end, the continuity of tangential components of the electric and magnetic field phasors across the planar interface

$z = 0$ yields the four conditions [17]

$$\left. \begin{aligned} \alpha_{A1}A_{A1} - \alpha_{A2}A_{A2} &= i\alpha_{B1} \sin \psi A_{B1} + \alpha_{B1}^2 \cos \psi A_{B2} \\ \kappa_R A_{A1} + \kappa_L A_{A2} &= -i\alpha_{B1} \cos \psi A_{B1} - \varepsilon_B^s \sin \psi A_{B2} \\ -i\sqrt{\frac{\varepsilon_A}{\mu_A}} (\alpha_{A1}A_{A1} + \alpha_{A2}A_{A2}) &= \sqrt{\frac{\varepsilon_0}{\mu_0}} (\alpha_{B1}^2 \cos \psi A_{B1} - i\alpha_{B2} \varepsilon_B^s \sin \psi A_{B2}) \\ -i\sqrt{\frac{\varepsilon_A}{\mu_A}} (\kappa_R A_{A1} - \kappa_L A_{A2}) &= \sqrt{\frac{\varepsilon_0}{\mu_0}} (-\varepsilon_B^s \sin \psi A_{B1} + i\alpha_{B2} \varepsilon_B^s \cos \psi A_{B2}) \end{aligned} \right\}, \quad (22)$$

which are represented compactly as

$$[N] \cdot \begin{bmatrix} A_{A1} \\ A_{A2} \\ A_{B1} \\ A_{B2} \end{bmatrix} = \begin{bmatrix} 0 \\ 0 \\ 0 \\ 0 \end{bmatrix}. \quad (23)$$

The 4×4 matrix $[N]$ must be singular for surface-wave propagation. The dispersion equation $\det [N] = 0$ reduces to the equation

$$\begin{aligned} &\alpha_{B1} [2\sqrt{\varepsilon_A \mu_A} (\kappa_L \kappa_R \alpha_{B1}^3 + \varepsilon_B^s \alpha_{A1} \alpha_{A2} \alpha_{B2}) + \alpha_{B1} (\kappa_L \alpha_{A1} + \kappa_R \alpha_{A2}) (\varepsilon_A \alpha_{B1} + \varepsilon_B^s \mu_A \alpha_{B2})] \cos^2 \psi \\ &- \varepsilon_B^s \{ [2\sqrt{\varepsilon_A \mu_A} (\kappa_L \kappa_R \alpha_{B1} \alpha_{B2} + \varepsilon_B^s \alpha_{A1} \alpha_{A2}) + (\kappa_L \alpha_{A1} + \kappa_R \alpha_{A2}) (\varepsilon_A \alpha_{B1} + \varepsilon_B^s \mu_A \alpha_{B2})] \sin^2 \psi \\ &- \sqrt{\varepsilon_A \mu_A} (\kappa_L \alpha_{A1} - \kappa_R \alpha_{A2}) \alpha_{B1} (\alpha_{B1} - \alpha_{B2}) \sin 2\psi \} = 0. \end{aligned} \quad (24)$$

After extracting q from Eq. (24), generally by numerical means, the relative values of the four scalars $A_{A1,2}$ and $A_{B1,2}$ can be determined from Eq. (23) by straightforward algebraic manipulations.

3.2 Numerical studies

As in Sec. 2.2, we fix partnering material \mathcal{A} by selecting the relative constitutive parameters $\varepsilon_A = 2.6724 - 0.0007i$, $\xi_A = 0.0652 + 0.0005i$ and $\mu_A = 0.9642 + 0.0001i$. Let us start with the case where the relative permittivity parameters of material \mathcal{B} , namely ε_B^s and ε_B^t , have negative-valued real parts and positive-valued imaginary parts. Specifically, let $\varepsilon_B^s = -12 + 0.0045i$ and $\varepsilon_B^t = -8 + 0.005i$. Thus, material \mathcal{B} behaves like an anisotropic plasmonic material that exhibits a modest degree of dissipation. The corresponding surface waves are akin to SPP waves. In Fig. 4, the real and imaginary parts of q are plotted against orientation angle ψ for the solitary (complex-valued) q solution emerging from the dispersion equation (24). The real part of q is almost independent of ψ . In contrast, the imaginary part of q oscillates as ψ increases such that $\text{Im}\{q\} > 0$ for $\psi \in (0^\circ, 64^\circ) \cup (170^\circ, 180^\circ)$ and $\text{Im}\{q\} < 0$ for $\psi \in [64^\circ, 170^\circ]$. Therefore, for certain orientations of material \mathcal{B} the surface wave is attenuated as it propagates while for other orientations it is amplified as it propagates. Furthermore, at two specific orientations of material \mathcal{B} the surface wave propagates with neither attenuation nor amplification. A similar simultaneous amplification/attenuation phenomenon has been reported for SPP waves guided by the planar interface of a metal and a uniaxial dielectric material [24].

Lastly, we turn to the case where the relative permittivity parameters of material \mathcal{B} have positive-valued real parts and positive-valued imaginary parts. Specifically, let $\varepsilon_B^s = 2 + i$ and $\varepsilon_B^t = 3 + 1.5i$. Thus, material \mathcal{B} behaves like an anisotropic dielectric material that exhibits dissipation. The corresponding surface waves are akin to Dyakonov waves [6, 8]. Unlike the case represented in Fig. 4, the dispersion equation (24) here yields two, one or no q solutions, depending upon the value of ψ . The real and imaginary parts of q are plotted against ψ for all solutions in Fig. 5. Specifically, we found two q solutions for $23^\circ < \psi < 76^\circ$, one q solution for $14^\circ < \psi < 23^\circ$ and $76^\circ < \psi < 90^\circ$, and no q solution at all for $0^\circ < \psi < 14^\circ$. The existence of two solutions signifies a marked difference from the case for conventional Dyakonov waves [1]. In the case represented in Fig. 5 all surface-wave solutions are attenuated regardless of the orientation angle ψ , which contrasts with a simultaneous amplification/attenuation phenomenon that has been reported for Dyakonov waves guided by the planar interface of an isotropic dielectric material and a uniaxial dielectric

material [25]. Also, the existence of two surface waves at each orientation for $23^\circ < \psi < 76^\circ$ in Fig. 5 contrasts with the usual case for Dyakonov waves in which the dispersion equation admits only one solution for each propagation direction [9].

4 Closing remarks

Electromagnetic surface waves supported by an isotropic chiral material were investigated numerically via the associated canonical boundary-value problem. In the case where the partnering material was an isotropic dielectric material, surface waves akin to SPP waves were excited; while in the case where the partnering material was a uniaxial dielectric material, surface waves akin to Dyakonov waves and SPP waves were excited. By selecting an isotropic chiral material capable of simultaneously supporting attenuation and amplification of plane waves, depending upon circular polarization state, the amplitudes of the SPP-like waves could be either amplified or attenuated, depending upon the relative permittivity of the isotropic dielectric partnering material or the direction of propagation relative to the optic axis of the uniaxial dielectric partnering material. Therefore, wider opportunities for surface-wave propagation are supported by isotropic chiral materials, as compared to achiral materials in analogous scenarios.

Acknowledgment JN is supported by a Deans' Vacation Scholarship (University of Edinburgh).

References

- [1] J.A. Polo Jr., T.G. Mackay, A. Lakhtakia, *Electromagnetic Surface Waves: A Modern Perspective*, Elsevier, 2013.
- [2] J.M. Pitarke, V.M. Silkin, E.V. Chulkov, P.M. Echenique, Theory of surface plasmon and surface-plasmon polaritons, *Rep. Prog. Phys.* 70 (20017) 1–87.
- [3] S.A. Maier, *Plasmonics: Fundamentals and Applications*, Springer, 2007.
- [4] J. Homola (Ed.), *Surface Plasmon Resonance Based Sensors*, Springer, 2006.
- [5] I. Abdulhalim, M. Zourob, and A. Lakhtakia, Surface plasmon resonance for biosensing: A mini-review, *Electromagnetics* 28 (2008) 214–242.
- [6] M.I. D'yakonov, New type of electromagnetic wave propagating at an interface, *Sov. Phys. JETP* 67 (1988) 714–716.
- [7] D.B. Walker, E.N. Glytsis, T.K. Gaylord, Surface mode at isotropic-uniaxial and isotropic-biaxial interfaces, *J. Opt. Soc. Am. A* 15 (1998) 248–260.
- [8] O. Takayama, L. Crasovan, D. Artigas, L. Torner, Observation of Dyakonov surface waves, *Phys. Rev. Lett.* 102 (2009) 043903.
- [9] O. Takayama, L.-C. Crasovan, S.K. Johansen, D. Mihalache, D. Artigas, L. Torner, Dyakonov surface waves: A review, *Electromagnetics* 28 (2008) 126–145.
- [10] A. Lakhtakia, *Beltrami Fields in Chiral Media*, World Scientific, 1994.
- [11] D.N. Pattanayak and J.L. Birman, Wave propagation in optically active and magnetoelectric media of arbitrary geometry, *Phys. Rev. B* 24 (1981) 4271–4278.
- [12] N. Engheta, P. Pelet, Surface waves in chiral layers. *Opt. Lett.* 16 (1991) 723–725.

- [13] A.N. Fantino, Planar interface between a chiral medium and a metal: surface wave excitation, *J. Mod. Opt.* 43 (1996) 2581–2593.
- [14] G. Pellegrini, M. Finazzi, M. Celebrano, L. Duò, P. Biagioni, Chiral surface waves for enhanced circular dichroism, *Phys. Rev. B* 95 (2017) 241402(R).
- [15] T.G. Mackay, A. Lakhtakia, Simultaneous amplification and attenuation in isotropic chiral materials, *J. Opt. (UK)* 18 (2016) 055104.
- [16] B.Y.-K. Hu, Kramers–Kronig in two lines, *Am. J. Phys.* 57 (1989) 821.
- [17] H.C. Chen, *Theory of Electromagnetic Waves*, McGraw–Hill, 1983.
- [18] T.G. Mackay, A. Lakhtakia, *Modern Analytical Electromagnetic Homogenization*, Morgan & Claypool, 2015.
- [19] T.G. Mackay, A. Lakhtakia, Dynamically controllable anisotropic metamaterials with simultaneous attenuation and amplification, *Phys. Rev. A* 92 (2015) 053847.
- [20] U. Fano, The theory of anomalous diffraction gratings and of quasi-stationary waves on metallic surfaces (Sommerfeld’s waves), *J. Opt. Soc. Am.* 31 (1941) 213–222.
- [21] D. Bohm, E.P. Gross, Theory of plasma oscillations. A. Origin of medium-like behavior, *Phys. Rev.* 75 (1949) 1851–1864.
- [22] D. Bohm, E.P. Gross, Theory of plasma oscillations. B. Excitation and damping of oscillations, *Phys. Rev.* 75 (1949) 1864–1876.
- [23] M. Born, E. Wolf, *Principles of Optics*, 7th (expanded) Edn., Cambridge Univ. Press, 1999.
- [24] T.G. Mackay, A. Lakhtakia, Simultaneous existence of amplified and attenuated surface-plasmon-polariton waves, *J. Opt. (India)* (2018) <https://doi.org/10.1007/s12596-018-0481-y>.
- [25] T.G. Mackay, A. Lakhtakia, Simultaneous existence of amplified and attenuated Dyakonov surface waves, *Opt. Commun.* 427 (2018) 175–179.

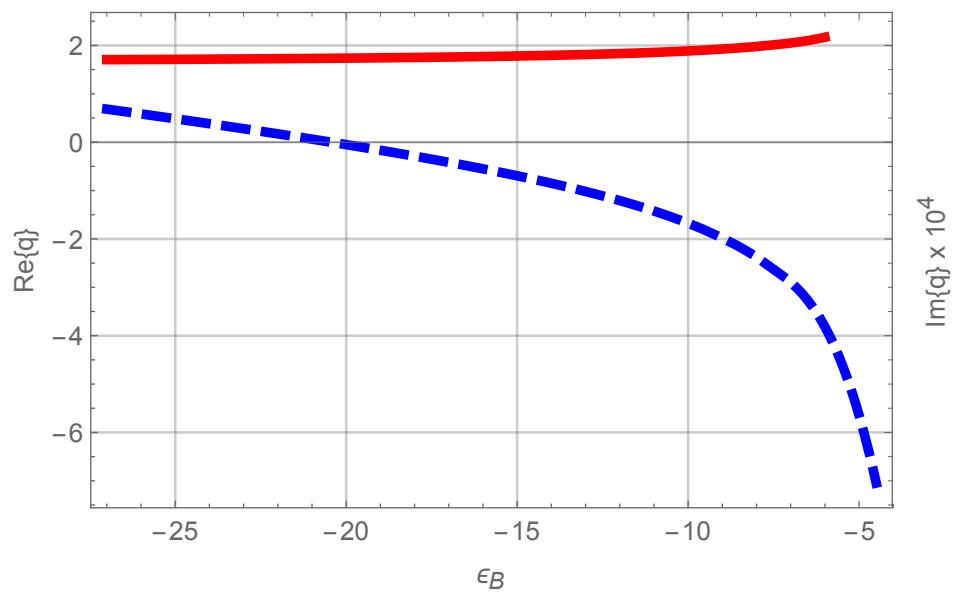


Figure 1: $\text{Re}\{q\}$ (red solid curve) and $\text{Im}\{q\}$ (blue dashed curve) plotted against ϵ_B .

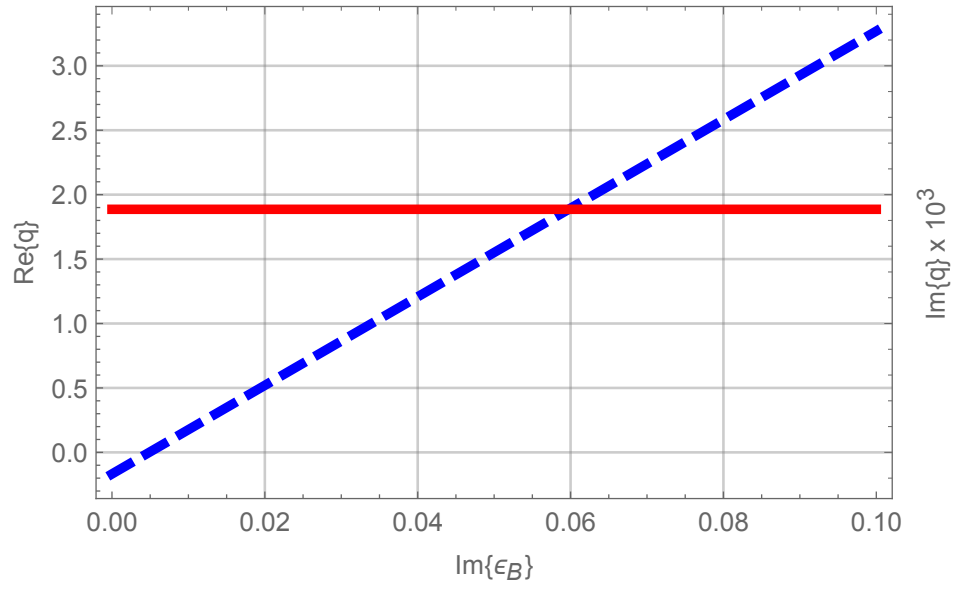


Figure 2: $\text{Re}\{q\}$ (red solid curve) and $\text{Im}\{q\}$ (blue dashed curve) plotted against $\text{Im}\{\varepsilon_B\}$ with $\text{Re}\{\varepsilon_B\} = -10$.

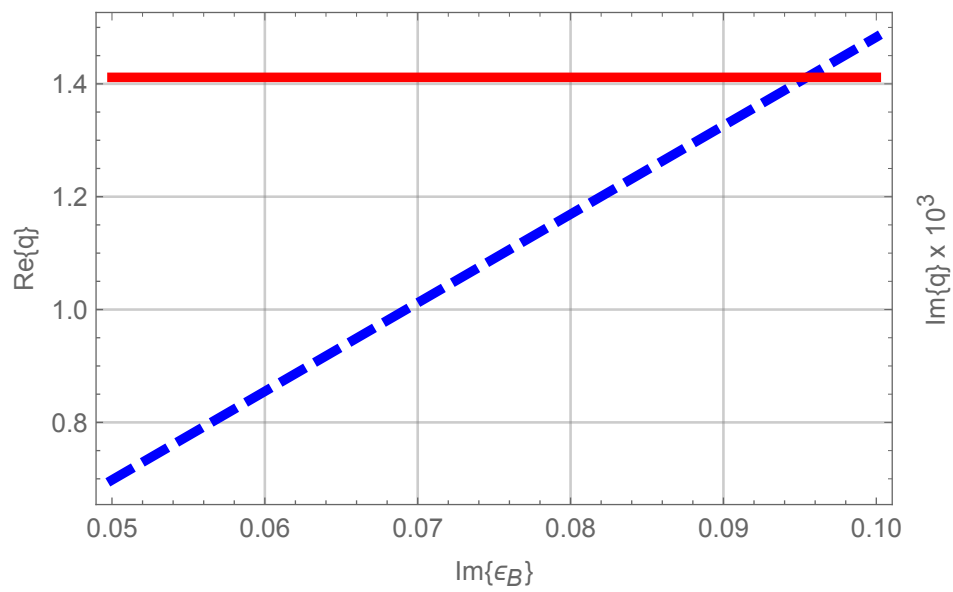


Figure 3: As Fig. 2 except that $\text{Re}\{\epsilon_B\} = 10$.

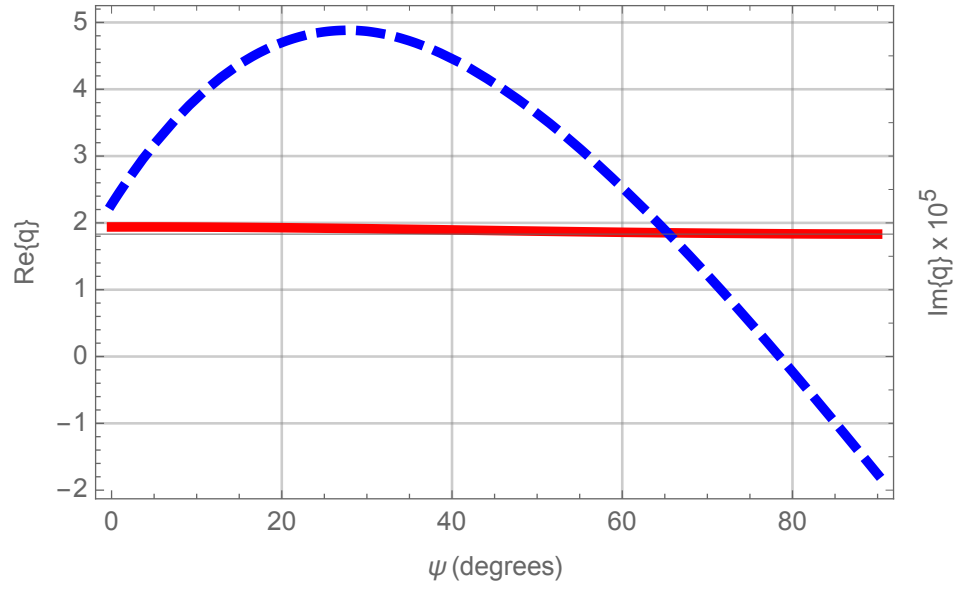


Figure 4: $\text{Re}\{q\}$ (red solid curve) and $\text{Im}\{q\}$ (blue dashed curve) plotted against orientation angle ψ with $\epsilon_B^s = -12 + 0.0045i$ and $\epsilon_B^t = -8 + 0.005i$.

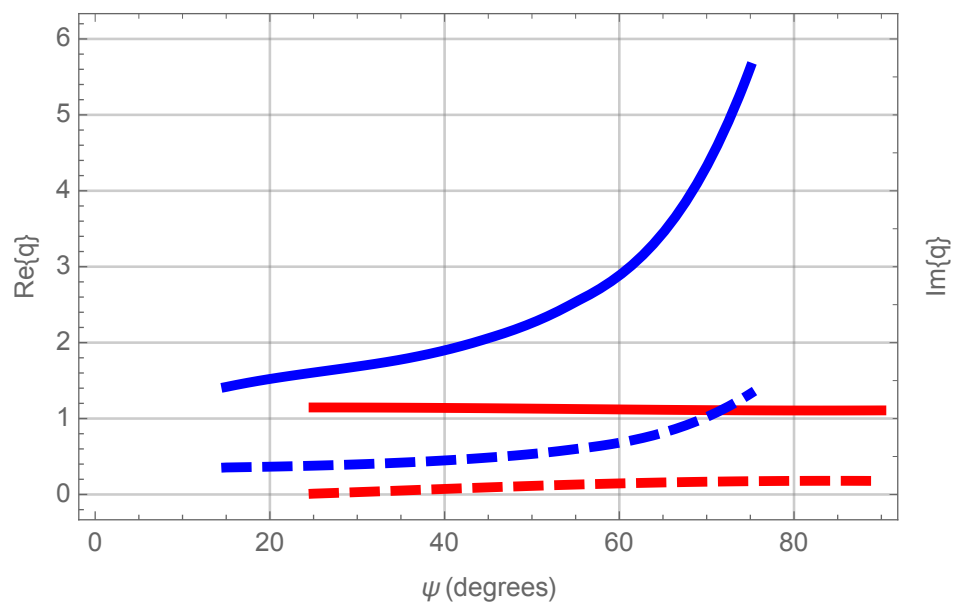


Figure 5: As Fig. 4 except that $\epsilon_B^s = 2 + i$ and $\epsilon_B^t = 3 + 1.5i$.